

FINAL TECHNICAL REPORT

Award Number 1434-HQ-97-GR03161

Recipient: San Diego State University Foundation
5178 College Avenue
San Diego, California 92182-1020

PI.: Steven M. Day
San Diego State University
Department of Geological Sciences
San Diego, California 92182-1900

Project title: Dynamic Rupture Model of Thrust and Strike-Slip Fault
Interactions in the Los Angeles Basin

Program Element III

Research supported by the U.S. Geological Survey (USGS), Department of the Interior, under USGS award number 1434-HQ-97-GR03161. The views and conclusions contained in this document are those of the authors and should not be interpreted as necessarily representing the official policies, either expressed or implied, of the U.S. Government.

**DYNAMIC RUPTURE MODEL OF THRUST AND STRIKE-SLIP
FAULT INTERACTIONS IN THE LOS ANGELES BASIN**

Steven Day
office (619) 594-2663
fax (619) 594-4372
email day@moho.sdsu.edu

San Diego State University
Department of Geological Sciences
San Diego, California 92182-1020

TECHNICAL ABSTRACT

Earthquake magnitude is determined by rupture area. Thrust faults beneath the Los Angeles basin are offset, and thus segmented, by strike-slip faults. The objective of this work is to develop models of dynamic rupture sufficiently realistic to provide useful estimates of the likelihood of multiple segments of this fault system rupturing in a single earthquake. In a previous one-year effort, we developed and tested a 2D finite difference method for the dynamic simulation of rupture of parallel thrust faults offset by strike-slip segments. Under the current one-year effort we have completed the following: (1) Development and testing of a 3D finite difference code for modeling the rupture dynamics of segmented thrust faults. The method includes intersecting thrust and strike-slip ("tear fault") segments. (2) Sensitivity study of segmented thrust rupture in 2D. (3) Sensitivity study of segmented thrust rupture in 3D. (4) Completion of a 3D numerical simulation study of multi-segment ruptures on strike-slip fault systems (with R. Harris of the USGS). (5) Completion and publication of a study of seismological constraints on fault zone friction laws (with D. Wald of the USGS and G. Yu)

Results of 3D simulations (using 10 km long thrust fault segments and typical fault strength and stress drop values) indicate that, if the thrust segments are linked by a tear fault, rupture can jump segment offsets several km. In contrast, in the absence of a linking tear fault, offsets of only a few hundred meters become a barrier to rupture. The segment boundaries of Los Angeles area thrust fault segmentation models consist of offsets of up to about 5 km. Some of the offsets are occupied by lateral ramps and tear faults defined by surface fault traces or seismological observations. For blind thrusts, some of the fault offsets are inferred from offsets in the fold axes above the thrusts, and the presence of lateral ramps and tear faults is uncertain. Since the presence of a tear fault or lateral ramp linking offset thrust fault segments greatly abets multi-segment rupture, it is critical to accurately characterize the nature of the thrust fault segment offsets.

PREFACE

This final technical report is a compilation of three documents reporting progress in modeling the rupture dynamics of segmented fault systems.

Part I describes work performed in collaboration with Ruth Harris of the U.S.G.S. to investigate 3D effects in the rupture of segmented strike slip faults. Finite difference computations are used to perform 3D simulations of spontaneous rupture propagation on segmented strike-slip faults. These numerical simulations show how some earthquakes may cascade into multi-segment events, whereas others may be stopped by the geometrical complexity. Our simulations provide a physical basis to assess the likelihood of future cascade earthquakes, given seismological and geological information on fault zone geometry and slip history. Whether or not a rupture can jump across a narrow stepover will depend on a number of factors, including the strength and stress distribution and the geometry of the stepover, as demonstrated by our examples. Alternatively, our 3D physical models demonstrate that wide stepovers (>5 km) will very rarely be jumped during an earthquake. Part I has been submitted for publication in *Geophysical Research Letters* (R. A. Harris and S. M. Day).

Part II describes a dynamic model for rupture of a segmented thrust fault. Finite difference simulations in 2D and 3D are used to investigate the potential for multi-segment cascade ruptures to occur. The simulations extend the methods developed and applied in Part I, in that they include orthogonal, intersecting faults to model the interaction of the thrust fault segments with the tear fault. For reasonable assumptions for fault segment length, strength, and stress drop, rupture can jump offsets of up to 2 km if a tear fault is present, consistent with observations of well studied thrust earthquakes. Absent a tear fault, the maximum offset that can be breached is an order of magnitude smaller. Part II has been submitted for publication in *Geophysical Research Letters* (H. Magistrale and S. M. Day).

Part III describes a test of alternative hypotheses about fault zone rheology. We investigated three large earthquakes in this study: the 1992 Landers earthquake, the 1994 Northridge earthquake, and the 1995 Kobe earthquake. The slip time histories determined from near-source ground motions, teleseismic waves, and geodetic displacement by Wald and others were used in reconstruction of stress time histories on the fault planes. Results for the three events suggest that the dynamic stress drops on the fault plane occur monotonically after passage of the rupture front. The large stress drops are localized in small areas, surrounded by low, and often negative, stress drop regions. The stress time histories show no evidence of a self-healing mechanism, and short rise times can be explained by stress drop heterogeneity on the fault plane. Part III has been published in the *Bulletin of the Seismological Society of America* (S. M. Day, G. Yu, and D. Wald).

PUBLICATIONS

Harris, R. A., and S. M. Day (1997). Effects of a low-velocity zone on a dynamic rupture, *Bull. Seism. Soc. Am.*, 87, pp. 1267-1280.

Day, S.M., G. Yu, and D. Wald (1998). Dynamic stress changes during earthquake rupture, *Bull. Seism. Soc. Am.*, 88, 512-522.

Harris, R.A., and S.M. Day (1998). Dynamic 3D simulations of earthquakes on en echelon faults, submitted to *Geophysical Research Letters*.

Magistrale, H., and S.M. Day (1998). Three dimensional simulation of multi-segment thrust fault rupture, submitted to *Geophysical Research Letters*.

PART I

DYNAMIC 3D SIMULATIONS OF EARTHQUAKES ON EN ECHELON FAULTS

DYNAMIC 3D SIMULATIONS OF EARTHQUAKES ON EN ECHELON FAULTS

Ruth A. Harris* and Steven M. Day†

**Manuscript submitted to Geophysical Research Letters
October 1998**

***U.S. Geological Survey, Mail Stop 977, 345 Middlefield Rd, Menlo Park,
CA 94025**

**†Department of Geological Sciences, San Diego State University, San
Diego, CA 92182**

One of the mysteries of earthquake mechanics is why earthquakes stop. This process determines the difference between small and devastating ruptures. One possibility is that fault geometry controls earthquake size. We test this hypothesis using a numerical algorithm and apply our knowledge to two California fault zones. We find that the size difference between the 1934 and 1966 Parkfield, California, earthquakes may be the product of a stepover at the southern end of the 1934 earthquake and show how the 1992 Landers, California, earthquake followed physically reasonable expectations when it jumped across en echelon faults to become a large event.

The 1992 Landers earthquake initiated on one fault, then jumped across numerous geometrical boundaries to rupture through at least 4 more faults, becoming a $M_w 7.3$ event^{1,2} (Fig. 1). The resulting surface rupture of the 1992 earthquake has been mapped in detail. Although the probability of one earthquake cascading into another has been included in some hazard models³, what stops earthquakes after they begin rupturing is unknown. Some have suggested the eventual magnitude is determined at the start of rupture⁴. Others propose that material properties of the fault zone region stop earthquake propagation^{5,6}. A third hypothesis⁷⁻¹⁵, which is investigated in this work, is that features such as branches, bends, and steps in faults may control how far an earthquake can dynamically propagate, and its eventual magnitude.

Geometrical discontinuities in faults are commonly observed at the earth's surface by geological field investigators^{7,9,10,16}. Deeper studies of the earth's crust, using techniques such as fault-zone guided waves¹⁷ and foreshock and aftershock locations^{18,19} have also suggested that some of the geometrical discontinuities observed at the earth's surface extend to seismogenic depths. We thus examine how these fault zone complexities might control earthquake size.

We modify a 3-D finite-difference computer program²⁰ to simulate spontaneously propagating cracks (simulated earthquakes) on an echelon vertical strike-slip faults (Fig. 2). To ensure that the stresses remain finite at the front of the propagating crack, and are thereby 'stoppable' we employ a slip-weakening fracture criterion²⁰⁻²³. This fracture criterion is based on dynamic slip-events in rock samples in the laboratory²⁴ and modeling of strong-motion seismograms recorded in the field²⁵⁻²⁷.

We nucleate a simulated earthquake on a fault plane by starting at one 'nucleation point', then forcing the rupture to propagate outward at approximately one-half the shear-wave speed of the medium. During this time, the stress is gradually dropped from its initial magnitude down to the dynamic friction stress. As soon as the rupture has enough energy to propagate spontaneously (by itself) it is allowed to do so. The size of the artificial nucleation process is controlled by a number of factors, including the slip-weakening critical distance, d_0 , and the proximity of the initial stresses to failure^{20,23}. Fortunately, the nucleation region is often small compared to the overall rupture extent on the first fault plane, and the rest of the rupture process is unaffected.

After the spontaneous rupture is underway, there is a range of possible outcomes. Among these are: 1) The simulated earthquake rupture can propagate along one fault, then run out of energy and cease propagating along this fault. In this scenario, the earthquake may not even reach the earth's surface. This case often occurs in nature and results in a single-fault earthquake. 2) The earthquake can reach the earth's surface, but then stops propagating along strike of the fault. This is also observed in large earthquakes. 3) The earthquake can propagate to the end of one fault, then jump across a fault segment boundary to another, an echelon fault, thereby continuing on its propagation path, as occurred during the 1992 Landers earthquake².

We simulate the range of events described in the foregoing and examine the conditions that lead to each circumstance. We start with a homogeneous strength distribution along-strike and along-dip of the first fault plane, and with stress conditions that lead to overall subshear rupture propagation speeds (slower than the shear-wave speed of the material). Here we incorporate homogeneous bulk material properties (material velocities, densities, and shear moduli) in the vicinity of the faults, but allow the faults' frictional strength to vary. Although the use of material heterogeneity^{28,29} can add complexity to our fault zone models, we confine our analysis to as few variables as possible.

Our first simulation is of an earthquake nucleating near the bottom of a 30 km long x 15 km deep vertical strike-slip fault that intersects the earth's surface. A companion, parallel strike-slip fault lies 1 km away (stepover width), and overlaps the first fault by a few kilometers. We set the initial stress (shear and normal) conditions on the two faults to be homogeneous, to approximate a fault zone that last ruptured along its entire length (both faults) and depth, in one large earthquake. Table 1 summarizes the initial conditions.

We nucleate the rupture on one fault (fault 1), then let it propagate. Stress-waves are produced by the rupture and interact both with the surrounding crustal material and with portions of the rupture itself. The simulated earthquake first reaches the top of fault 1, the earth's surface, in 4.98 seconds, first reaches the end of fault 1 by 6.04 seconds, then ceases to propagate after reaching the extremities of fault 1. The dynamic stresses generated by the stress-waves are insufficient to permit the jump across the 1-km wide stepover. This simulated earthquake was contained by the geometrical complexity of the fault zone, and remained a single-fault event.

With a narrower stepover, of 0.75 km (Fig. 3), however, the simulated rupture jumps to the second fault segment. By 7.62 seconds, for the dilational stepover (7.32 seconds for a compressional stepover) the simulated earthquake is propagating on the second fault segment. An interesting feature of the simulated jump is that it occurs to a region on the

second fault (fault 2) that is near the earth's surface. This characteristic is a result of both normal and shear stress changes due to the stress waves and their enhancement by the free-surface effect.

In the preceding example the en echelon faults extend from the earth's surface down to 15 km depth. The along-strike length of the first fault is 15-km beyond the nucleation point, for a 30-km total length. The second fault is also 30 km long. In this example the maximum jump distance is 0.75 km. Deeper faults allow for slightly wider jumps if the nucleation point is also deeper, longer faults do not change the jump-distances significantly. These findings are for dilational stepovers. For compressional stepovers, longer faults allow jumps across slightly wider steps. The maximum jump distance, for a 50% increase in either fault length or fault depth, is 1.25 km.

Another geometrical feature that can be measured for en echelon stepovers is the amount of fault overlap. In 2D numerical studies the amount of overlap was important for determining the likelihood of a jump across a dilational fault stepover³⁰. In 3D, jumps across dilational steps also depend on the amount of overlap. If there is no overlap, then the rupture is unable to jump the 0.75 km wide dilational stepover, or even a narrower stepover 0.5 km-wide.

Next we examine varying strength as a function of depth. Weak near-surface material has been proposed for faults that exhibit shallow creep, either independently, or as a response to nearby disturbances³¹; weak material can also explain why many earthquakes generate little or no surface slip. In 3D homogeneous-strength simulations, however, it is difficult to slow a rupture on its path to a free surface. We follow Quin³² and employ a negative stress-drop region in a surficial layer ≥ 0.5 km in thickness to restrain rupture propagation to the ground surface. The simulated earthquake is then unable to jump the 0.75-km-wide stepover. We also test the effect of a weak zone below seismogenic depths,

where ductile creep may be occurring³¹ and find that it has no effect on whether or not the rupture jumps the fault stepover.

Stress conditions along strike may also not be homogeneous, as suggested by strong ground motion records^{25-27,33}. This may arise from material properties or rupture history. For example, the 1934 Parkfield, California earthquake (Fig. 1) was unable to jump across a fault stepover in the San Andreas fault, whereas the 1966 Parkfield earthquake jumped across the same fault stepover³⁴.

We model a Parkfield-like situation by taking the initial earthquake, with 2.4 MPa (24 bar) stress drop, as a preliminary event, which relaxed the first fault and perturbed the stress on the second fault (Fig. 4), which did not rupture coseismically. During the interseismic period, between earthquakes, an interseismic tectonic stress-increment occurs from deep slip on the San Andreas fault. The end result (simulated, but not shown in figure 4), which includes both the first earthquake's induced stress-changes and the interseismic tectonic stress-increment, is a subsequent 1966-like earthquake (2.4 MPa stress drop) that is able to jump the 1-km wide stepover.

Heterogeneous stress-distributions along strike and along depth may also lead to the jumping of wider stepovers such as where a previous earthquake breaks only a portion of the first fault. If the next earthquake also starts in this region it may be able to continue into a portion of the first fault that did not slip recently and therefore was closer to failure. Our modeling shows that earthquakes occurring on faults quite close to failure may jump wider stepovers, on the order of 3-4 km. This finding, that stress conditions quite close to failure can lead to much wider jumps was also observed with 2D simulations^{30,35}. Another condition that allows wider (3-4 km) stepovers to be jumped is a low-stress and low stress drop upper crust (1-3 km deep) overlying a higher stress and stress drop mid- and lower-crust.

The 1992 Landers earthquake jumped at least two stepovers during its northward progression. The southernmost stepover, that between the Johnson Valley and Homestead Valley faults, was bridged by the Landers (Kickapoo) fault that connected the two structures³⁶. Subsequently, the 2 km-wide, 5 km-overlap dilational stepover between the Homestead Valley and Emerson faults³⁷ was also unable to stop the 1992 earthquake. There doesn't appear to be a simple connecting structure at depth in this case³⁸, but from our numerical modeling efforts one can see that a jump of this width is not to be unexpected. Geologic trenching work (T. Rockwell, pers. communication) provides evidence that the Emerson fault only ruptures every other time the Homestead Valley fault ruptures. Once every 5000 years the Homestead Valley fault participates on its own, once every 10,000 years both rupture simultaneously. It is possible that, similar to Parkfield, the geometrical complexity controls how often the entire Landers fault zone ruptures and how often shorter, smaller magnitude events occur.

Our simple stepover model can be used to simulate the cascade potential of strike-slip earthquakes on en echelon faults. If we can assume that the crust surrounding faults behaves elastically during the time-period of an earthquake, and if we know that faults are not connected at depth, then it appears highly unlikely that an earthquake would jump a >5-km wide stepover. This appears true for both compressional and dilational stepovers and agrees with geological field observations^{13,39}.

We have presented the first 3D models of spontaneous rupture propagation on geometrically-complex strike-slip faults in an elastic medium. These numerical simulations show how some earthquakes may cascade into multi-segment events, whereas others may be stopped by the geometrical complexity. Our simulations provide a physical basis to assess the likelihood of future cascade earthquakes, given seismological and geological information on fault zone geometry and slip history. Whether or not a rupture can jump across a narrow stepover will depend on a number of factors, including the strength and

stress distribution and the geometry of the stepover, as demonstrated by our examples. Alternatively, our 3D physical models demonstrate that wide stepovers (>5 km) will very rarely be jumped during an earthquake. The cascade models for strike-slip faults can now be reframed.

References

1. Sieh, K.E. et al. Near-field investigations of the Landers earthquake sequence, April to July 1992, *Science*, **260**, 171-176 (1993).
2. Wald, D.J. & Heaton, T.H. Spatial and temporal distribution of slip for the 1992 Landers, California, earthquake, *Bull. Seism. Soc. Am.*, **84**, 668-691 (1994).
3. Jackson, D.D. et al. (Working Group on California Earthquake Probabilities) Seismic Hazards in southern California: Probable earthquakes 1994-2024, *Bull. Seism. Soc. Am.*, **85**, 379-439 (1995).
4. Ellsworth, W.L. & Beroza, G.C. Seismic evidence for a seismic nucleation phase, *Science*, **268**, 851-855 (1995).
5. Michael, A.J. & Eberhart-Phillips, D. Relations among fault behavior, subsurface geology, and three-dimensional velocity models, *Science*, **253**, 651-654 (1991).
6. Nicholson, C. & Lees, J.M. Travel-time tomography in the northern Coachella Valley using aftershocks of the 1986 ML 5.9 North Palm Springs earthquake, *Geophys. Res. Lett.*, **19**, 1-4 (1992).
7. Wallace, R.E. Earthquake recurrence intervals of the San Andreas fault, *Geol. Soc. Am. Bull.*, **81**, 2875-2890 (1970).
8. Schwartz, D. P. & Coppersmith, K. J. Fault behavior and characteristic earthquakes: examples from the Wasatch and San Andreas fault zones, *J. Geophys. Res.*, **89**, 5681-5698 (1984).
9. Sibson, R. H. Stopping of earthquake ruptures at dilational fault jogs, *Nature*, **316**, 248-251 (1985).
10. Sibson, R. H. Rupture interactions with fault jogs, in Earthquake Source Mechanics, Geophysical Monographs, Maurice Ewing Series, 6, American Geophysical Union, 157-167 (1986).
11. King, G.C.P. & Nabelek, J. L. Role of fault bends in the initiation and termination of rupture, *Science*, **228**, 984-987 (1985).

12. Wesnousky, S. G. Earthquakes, quaternary faults, and seismic hazard in California, *J. Geophys. Res.*, **91**, 12587-12631 (1986).
13. Barka, A. A. & Kadinsky-Cade, K. Strike-slip fault geometry in Turkey and its influence on earthquake activity, *Tectonics*, **7**, 663-684 (1988).
14. Aki, K. Geometric features of a fault zone related to the nucleation and termination of an earthquake rupture, *U.S. Geol. Surv. Open-File Rep.* **89-315**, 1-9 (1989).
15. Bouchon, M. & Streiff, D. Propagation of a shear crack on a nonplanar fault: a method of calculation, *Bull. Seism. Soc. Am.*, **87**, 61- 66 (1997).
16. Segall, P. & Pollard, D.D. Mechanics of discontinuous faults, *J. Geophys. Res.*, **85**, 4337-4350 (1980).
17. Li, Y.-G., Vidale, J. E., Aki, K. , Marone, C.J. & Lee, W.H.K. Fine structure of the Landers fault zone: segmentation and the rupture process, *Science*, **265**, 367-370 (1994).
18. Hauksson, E., Jones, L. M., Hutton, K. & Eberhart-Phillips, D. The 1992 Landers earthquake sequence: seismological observations, *J. Geophys. Res.*, **98**, 19835-19858 (1993).
19. Dodge, D.A., Beroza, G.C & Ellsworth, W.L. Foreshock sequence of the 1992 Landers, California, earthquake and its implications for earthquake nucleation, *J. Geophys. Res.*, **100**, 9865-9880 (1995).
20. Day, S. M. Three-dimensional simulation of spontaneous rupture: the effect of nonuniform prestress, *Bull. Seism. Soc. Am.*, **72**, 1881-1902 (1982).
21. Ida, Y. Cohesive force across the tip of a longitudinal shear crack and Griffith's specific surface energy, *J. Geophys. Res.*, **84**, 3796-3805 (1972).
22. Andrews, D. J. Rupture propagation with finite stress in antiplane strain, *J. Geophys. Res.*, **81**, 3575-3582 (1976a).
23. Andrews, D. J. Rupture velocity of plane strain shear cracks, *J. Geophys. Res.*, **81**, 5679-5687, (1976b).

24. Dieterich, J.D. Potential for geophysical experiments in large scale tests, *Geophys. Res. Lett.*, **8**, 653-656 (1981).
25. Beroza, G.C. & Mikumo, T. Short slip duration in the presence of heterogeneous fault properties, *J. Geophys. Res.*, **101**, 22449-22460 (1996).
26. Ide, S. & Takeo, M. Determination of constitutive relations of fault slip based on seismic wave analysis, *J. Geophys. Res.*, **102**, 27379-27391 (1997).
27. Day, S.M., Yu, G. & Wald, D.J. Dynamic stress changes during earthquake rupture, *Bull. Seism. Soc. Am.*, **88**, 512-522 (1998).
28. Andrews, D.J. & Ben-Zion, Y. Wrinkle-like slip pulse on a fault between different materials, *J. Geophys. Res.*, **102**, 553-571 (1997).
29. Harris, R.A. & Day, S.M. Effects of a low-velocity zone on a dynamic rupture, *Bull. Seism. Soc. Am.*, **87**, 1267-1280 (1997).
30. Harris, R.A. & Day, S.M. Dynamics of fault interaction: parallel strike-slip faults, *J. Geophys. Res.*, **98**, 4461- 4472 (1993).
31. Scholz, C.H. *The Mechanics of Earthquakes and Faulting* (Cambridge University Press, 1990).
32. Quin, H. Dynamic stress drop and rupture dynamics of the October 15, 1979 Imperial Valley, California, earthquake, *Tectonophysics*, **175**, 93-117 (1990).
33. Bouchon, M. The state of stress on some faults of the San Andreas system as inferred from near-field strong motion data, *J. Geophys. Res.*, **102**, 11731-11744 (1997).
34. Segall, P. & Du, Y. How similar were the 1934 and 1966 Parkfield earthquakes?, *J. Geophys. Res.*, **98**, 4527-4538 (1993).
35. Harris, R.A., Archuleta, R.J. & Day, S. M. Fault steps and the dynamic rupture process: 2-d numerical simulations of a spontaneously propagating shear fracture, *Geophys. Res. Lett.*, **18**, 893-896 (1991).

36. Sowers, J.M., Unruh, J. R., Lettis, W.R. & Rubin, T.D. Relationship of the Kickapoo fault to the Johnson Valley and Homestead Valley faults, San Bernardino County, California, *Bull. Seism. Soc. Am.*, **84**, 528-536 (1994).
37. Zachariasen, J. & Sieh, K. The transfer of slip between two en echelon strike-slip faults: A case study from the 1992 Landers earthquake, southern California, *J. Geophys. Res.*, **100**, 15281-15301 (1995).
38. Felzer, K.R. & Beroza, G.C. Deep structure of a fault discontinuity, submitted to *Geophysical Research Lett.*, July 1998.
39. Wesnousky, S. G. Seismological and structural evolution of strike-slip faults, *Nature*, **335**, 340-343 (1988).
40. Shedlock, K.M., Brocher, T.M. & Harding, S.R. Shallow structure and deformation along the San Andreas fault in Cholame Valley, California, based on high-resolution reflection profiling, *J. Geophys. Res.*, **95**, 5003-5020 (1990).
41. Harris, R.A. & Segall, P. Detection of a locked zone at depth on the Parkfield, California, segment of the San Andreas fault, *J. Geophys. Res.*, **92**, 7945-7962 (1987).
42. Eberhart-Phillips, D. & Michael, A.J. Three-dimensional structure, seismicity, and fault structure in the Parkfield region, central California, *J. Geophys. Res.*, **98**, 15737-15758 (1993).
43. Archuleta, R.J. & Day, S.M. Dynamic rupture in a layered medium: the 1966 Parkfield, earthquake, *Bull. Seism. Soc. Am.*, **70**, 671-689 (1980).

TABLE 1 Parameters used in the homogeneous simulations

Parameter	Value
P-wave velocity of the medium (m/s)	6000
S-wave velocity of the medium (m/s)	3464
Density of the medium (kg/m ³)	2670
Slip-weakening critical distance, d_0 (m)	0.10
Initial shear stress (MPa)	70
Initial normal stress, σ_{n0} (MPa)	120
Initial dynamic stress drop (MPa)	7
Static coefficient of friction, μ_s	0.677
Dynamic coefficient of friction, μ_d	0.525
Fracture energy, $G = d_0 \cdot \sigma_{n0} \cdot (\mu_s - \mu_d) / 4$ (J/m ²)	0.5×10^6

Figure Captions

Figure 1. a) Faults that ruptured during the 1992 M_w 7.3 Landers, California earthquake.

Inset, outline of California. Star is the location of the Landers earthquake, P is the location of Parkfield. Curved line is the San Andreas fault.

b) Mapped surface faults in the vicinity of the moderate 1934 and 1966 Parkfield, California earthquakes (modified from Shedlock et al.⁴⁰). Short-dash lines to the southwest of the San Andreas are the Southwest Fracture Zone, thought to be inactive⁴⁰.

Figure 2. En echelon vertical strike-slip faults. A right step in a right-lateral strike-slip fault is a dilational stepover (depicted). A left step would be a compressional stepover. The perpendicular distance between the two faults is the stepover width, the overlap distance is measured along-strike. The simulated earthquake is artificially nucleated in a region denoted by the star on the first fault plane, then allowed to spontaneously (unforced) propagate. Whether or not the earthquake can jump across the stepover between the faults depends on the fault geometry and the stress-conditions on the two faults.

Figure 3. Simulation of an earthquake that nucleates on a fault near a 0.75 km-wide dilational stepover. The initial stresses are assumed homogeneous over both 30-km long by 15-km deep fault planes. The material surrounding the faults is very strong so that the rupture cannot break into this 'intact rock'. After nucleation the rupture spontaneously propagates. The eight pictures show the amount of slip (contoured values) on each fault plane, at 1 second intervals, starting at 3 seconds after nucleation. The parameters for this simulation are given in Table 1. By 3 seconds (upper left), the rupture has propagated outward, but is still far from the earth's surface and the ends of the first fault. No slip has occurred on the second fault.

Soon after 5 seconds the rupture has reached the earth's surface, and by 6 seconds there is a significant amount of earth's-surface slip. By 7 seconds the rupture has reached the ends of the first fault, but slip still has not occurred on the second fault. By 8 seconds a very small patch of the second fault plane is slipping. The jump occurred at 7.6 seconds. At this point it is still not clear if the second fault will continue slipping. By 9 seconds however, a large patch is slipping on the second fault, and by 10 seconds, it is clear that this is a successful jump, since a significant portion of the second fault is slipping. If the stepover is widened, to 1-km, only the first fault ruptures and no jump occurs.

Figure 4. A rupture with a 2.4 MPa (24 bar) stress drop does not jump across the 1-km wide stepover, but does perturb the shear and normal stresses on the second fault plane (fault 2), as shown in this figure, a snapshot of the stress changes at 14 seconds. The resulting Coulomb stresses on fault 2 are contoured in MPa. Positive Coulomb stress (which occurs nowhere on fault 2, either now or earlier in time) would allow for rupture on the second fault, during either the coseismic or interseismic period. This simulation is the result of a very simplified model of the 1934 Parkfield earthquake, which does not include the tectonic stressing from the creeping section of the San Andreas fault northwest of Parkfield, or the complex pattern of interseismic stressing that occurs on the fault plane itself⁴¹. The 1 km stepover width⁴⁰ is consistent with seismicity modeling at Parkfield by Eberhart-Phillips and Michael⁴² (their figure 8). We select a 2.4 MPa stress drop for the 1934 earthquake based on the work of Archuleta and Day⁴³ for the 1966 Parkfield earthquake. To calculate the summed effects of the 1934 earthquake (shown above) and interseismic loading between the first (1934) and second (1966) quakes, we next add a 2.4 MPa increment in tectonic shear stress over both faults, then simulate the second (1966) earthquake. The result is that the simulated second earthquake (1966), which is also a 2.4 MPa (24 bar) stress

drop event, is able to jump the 1-km wide stepover. The distance along strike on fault 2 is measured from the nucleation point (star) on fault 1.

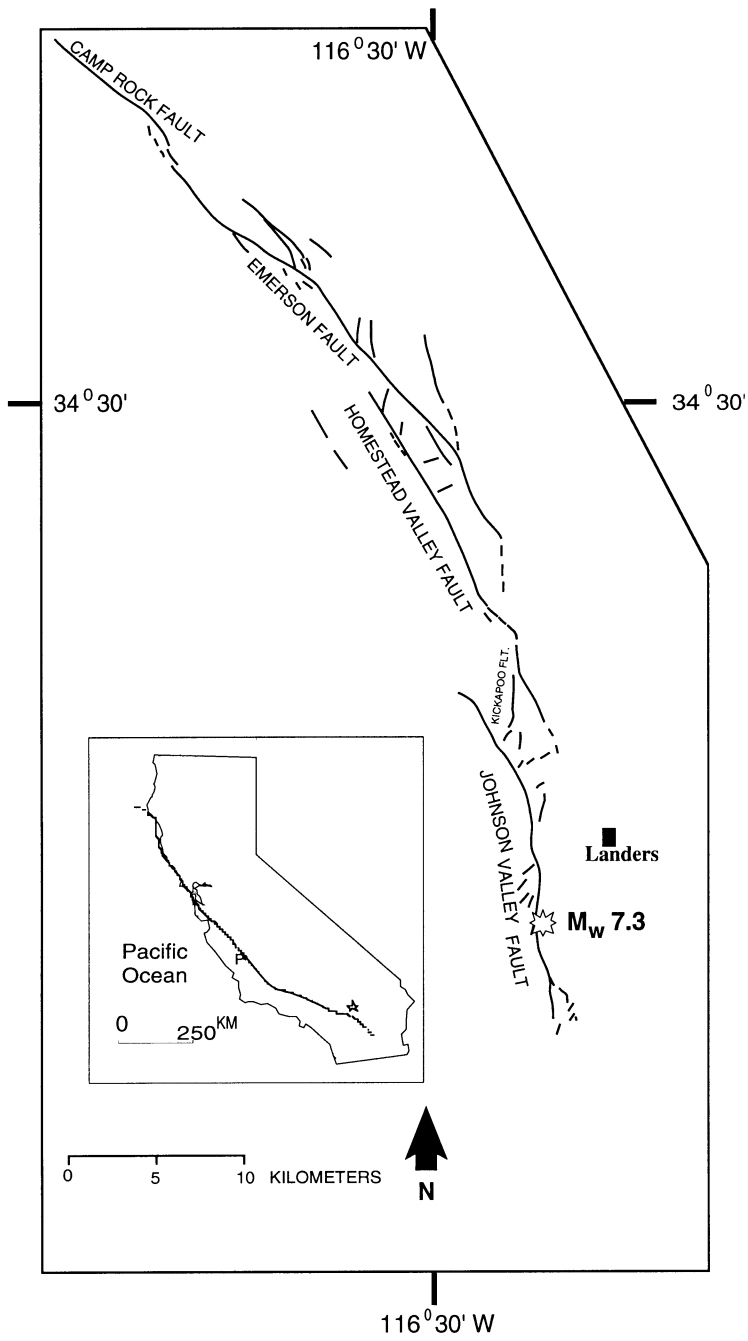


Figure 1a

Harris & Day

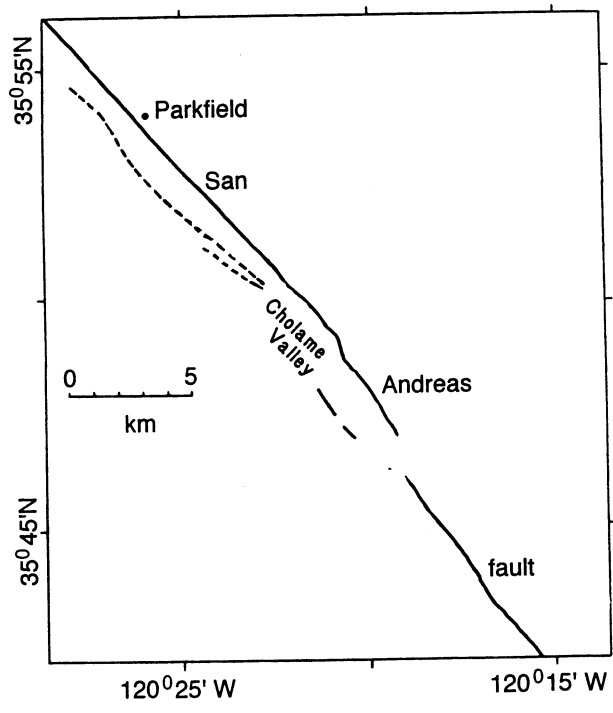


Figure 1b

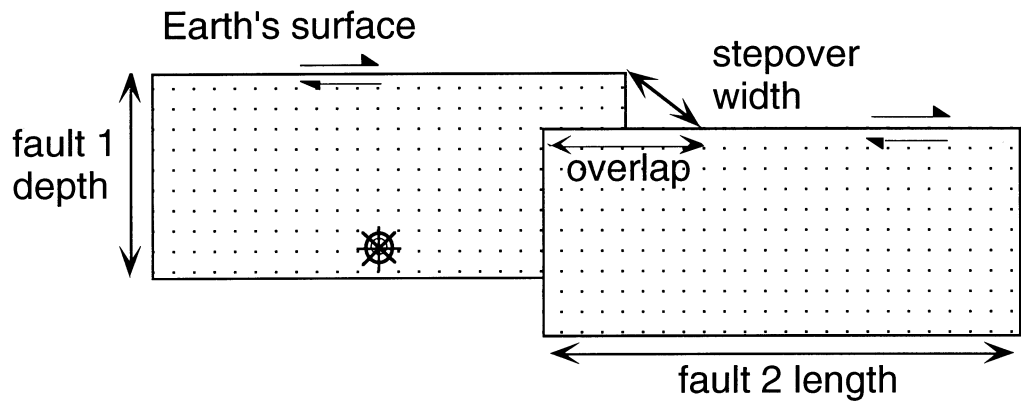


Figure 2

Harris & Day

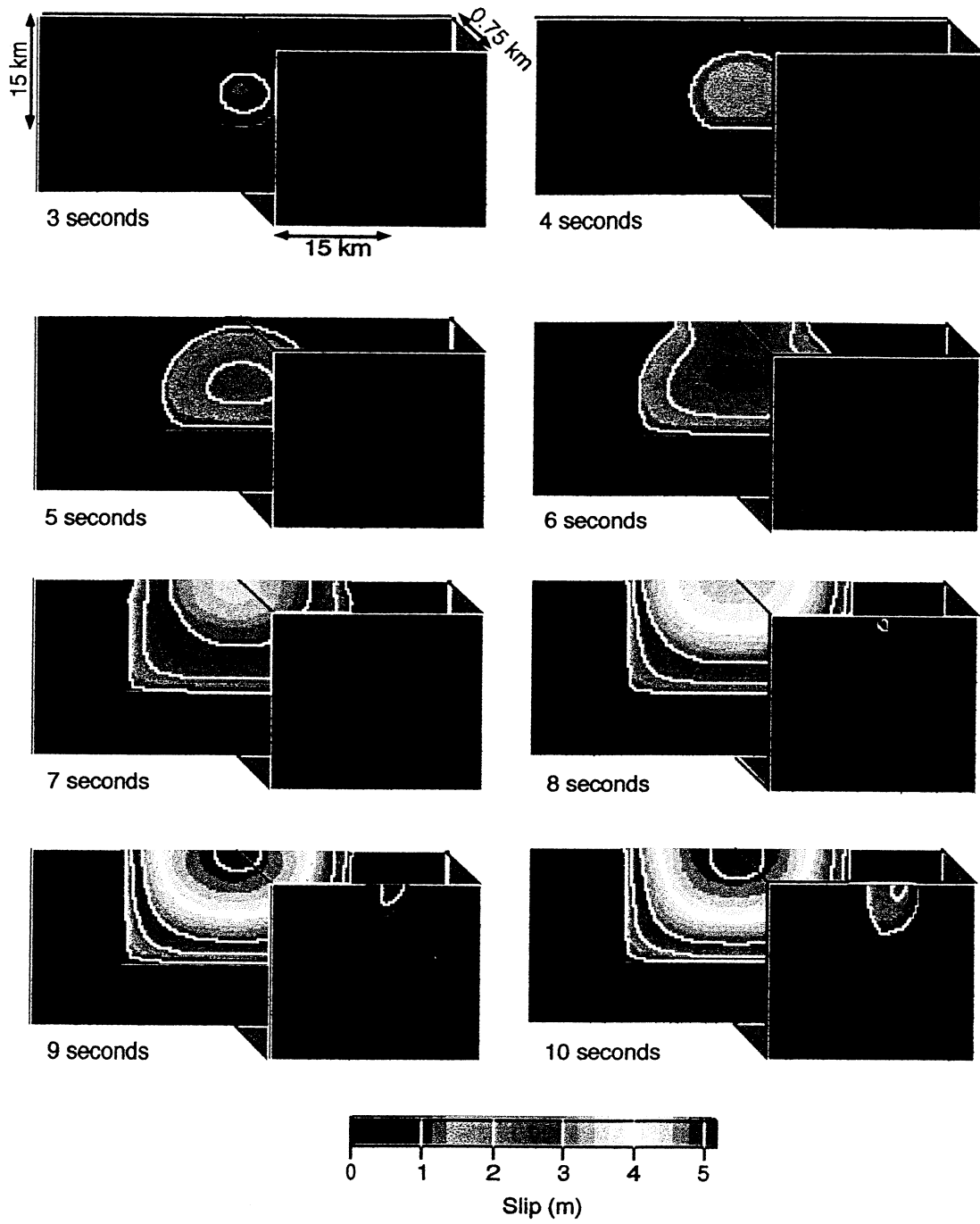


Figure 3

Harris & Day

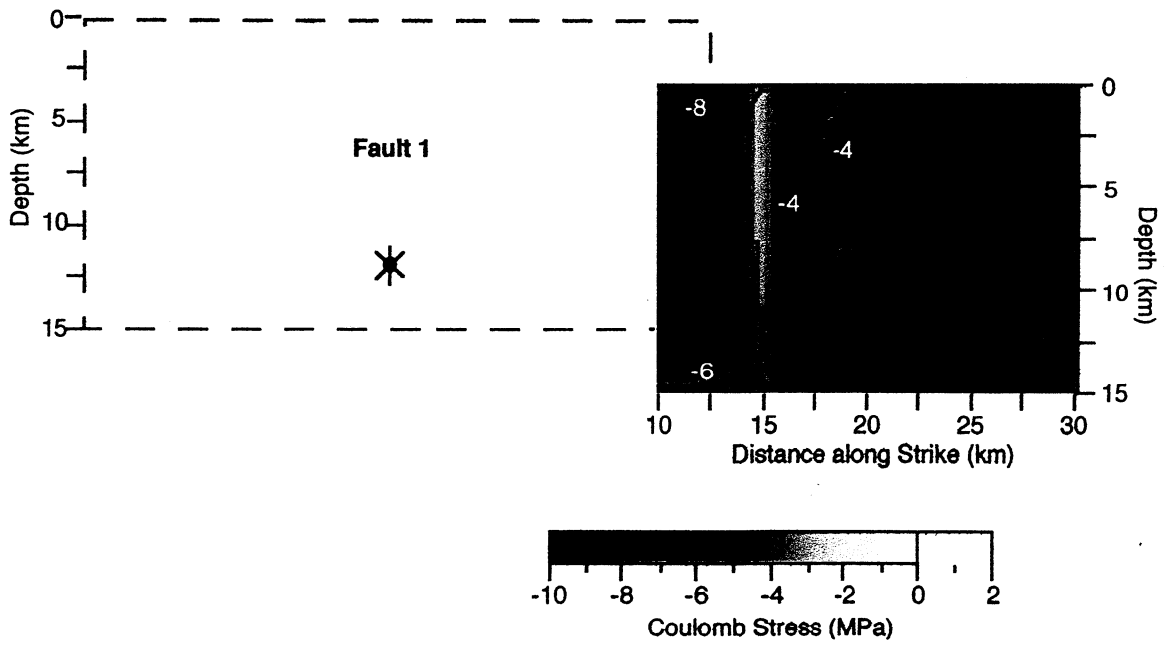


Figure 4
Harris & Day